

Accurate solutions of the Schrödinger and Dirac equations of H_2^+ , HD^+ , and HT^+ : With and without Born–Oppenheimer approximation and under magnetic field

Atsushi Ishikawa^a, Hiroyuki Nakashima^a, Hiroshi Nakatsuji^{a,b,*}

^aQuantum Chemistry Research Institute, JST-CREST, Kyodai Katsura Venture Plaza 106, Goryo Oohara 1-36, Nishikyo-ku, Kyoto 615-8245, Japan

^bInstitute of Multidisciplinary Research for Advanced Materials (IMRAM), Tohoku University, 2-1-1 Katahira, Aoba-ku, Sendai 980-8577, Japan

ARTICLE INFO

Article history:

Available online 17 September 2011

Keywords:

Schrödinger equation

Dirac equation

Free complement method

Accurate solutions

H_2^+

HD^+

HT^+

With and without Born–Oppenheimer approximation

Under magnetic field

ABSTRACT

We here give a review of our studies of hydrogen molecular ion (H_2^+) based on the accurate solutions of the Schrödinger equation (SE) and Dirac equations (DE) obtained by the free-complement (FC) methodology developed in our laboratory. We summarize the results of non-relativistic and relativistic studies of H_2^+ and its isotopomers HD^+ , and HT^+ , under the Born–Oppenheimer (BO) and non-BO treatments and with and without external magnetic field. H_2^+ is a simple one-electron molecule, and so has basic importance in quantum chemistry. Further, it is stable and of rich history of studies, particularly in interstellar science. For the non-relativistic SE, the convergence speed to the exact solution of the FC method is faster than that of the “exact” expansion, exhibiting high efficiency of the FC method. For the relativistic DE, not only accurate energy upper bounds but also lower bounds are calculated. The potential energy curves are also calculated at the non-relativistic and relativistic levels for all isotopomers, and chemically interesting information such as spectroscopic constants and transition frequencies are provided. The non-BO problem is also successfully solved for all isotopomers, and extremely accurate 1^1S and 1^3P energies, expectation values of interparticle distances are calculated for the ground and excited vibrational states. In the magnetic field calculation, our method is accurate in any strengths and any directions of the magnetic field. The gauge-origin problem is also investigated, and has shown that the gauge-origin dependence of the energy becomes smaller and smaller when the FC order is increased. All these results are clear example that the FC method combined with the variational principle gives very accurate analytical wave functions of H_2^+ in any cases and situations. Our investigations on H_2^+ and its isotopomers revealed the significant and accurate deterministic powers of the FC method in any situations of the problems: this methodology is reliable and stable to provide exact solutions for various types of non-relativistic and relativistic equations and problems appearing in the atomic and molecular physics and chemistry.

© 2011 Elsevier B.V. All rights reserved.

1. Introduction

Hydrogen molecular ion (H_2^+) is recognized as the simplest molecule. Despite of its simplicity, however, the physical and chemical studies of this molecule are surprisingly versatile. The primary reason lies in its simplicity; it consists of two nuclei and one electron. Further, H_2^+ is the only one example in which the exact “molecular” wave function is known. This is for the non-relativistic Schrödinger equation (SE) with the Born–Oppenheimer (BO) approximation. Owing to this, extensive theoretical works have been carried out for this molecule from the early times of the quantum chemistry. For example, various forms of wave function have been proposed for H_2^+ , ranging from an accurate wave function that has a similar

form to the exact wave function, to a simple LCAO–MO wave function [1–13]. Insights obtained with this molecule have been extended to larger molecules. Thus, H_2^+ has played a crucial role in the development of the quantum chemistry.

Not only theoretically, but also experimentally, H_2^+ has been extensively studied. For example, many works on vibrational–rotational spectrum of H_2^+ and its isotopomer HD^+ were carried out [1,2,14]. Experimental work on H_2^+ by pulse laser experiment was reported as a challenge of experimental accuracy ($\sim 10^{-2} \text{ cm}^{-1}$) for the dissociation energy [15]. H_2^+ is also interested in the field of astronomical physics and chemistry, because it is recognized as one of the most important interstellar molecules [16–27]. Theoretical works also played important roles on this issue, since highly accurate results are necessary for the assignment of astronomical spectroscopy. Thus, H_2^+ molecule has provided an excellent playground for both theoretical and experimental physicists and chemists in terms of the comparisons between theoretical and experimental results.

* Corresponding author at: Quantum Chemistry Research Institute, JST-CREST, Kyodai Katsura Venture Plaza 106, Goryo Oohara 1-36, Nishikyo-ku, Kyoto 615-8245, Japan.

E-mail address: h.nakatsuji@qcri.or.jp (H. Nakatsuji).

When fine detailed comparisons to experimental results are intended, many physical effects not included in the primitive SE in the BO approximation should be taken into account; relativistic effects, adiabatic or non-BO corrections, finite nuclear mass effect, quantum electrodynamics (QED) effects, and so on. Among them, leading terms are the relativistic and the non-BO corrections. Unfortunately, the exact wave functions of the Dirac equation (DE) and the non-BO SE are not known.

Many relativistic calculations on H_2^+ were made, not only by the variational method but also numerical methods like the finite difference method or the finite element method [28–35]. Major emphasis was on the accuracy of the calculated energy and quite accurate results were obtained. However, the analytical expression of the relativistic wave function was rather insufficient.

The non-BO problem of H_2^+ , i.e. solving the SE without the BO approximation is also very active area for theoretical study. The quantum effect of nuclear motion could be significant for H_2^+ because it consists of the lightest nuclei. There are various high precision calculations of H_2^+ with the non-BO Hamiltonian [36–44]. However, although their basis functions showed very rapid convergence to the exact solution, it is difficult to handle and generalize their functions for general molecules because their functions are arbitrary and complicated. Furthermore, the optimizations of large number of non-linear parameters are necessary for these types of wave functions, which often lead to extensive computational cost.

Another interesting example associated with H_2^+ is the effect of external magnetic field. This is also the case where the exact wave function is not known. A great deal of motivation for studying such strong magnetic fields comes from astronomical interests; extremely strong (10^{12} – 10^{15} G) magnetic fields are observed in the vicinity of astrophysical objects such as neutron stars or magnetar. In fact, recent X-ray data have revealed certain irregularities in the spectrum of a neutron star, and these can be interpreted as due to absorptions by interstellar atoms or molecules [17–27]. Aside from astrophysical viewpoints, atoms and molecules in magnetic fields are also interesting from theoretical atomic/molecular physics or chemistry [45–55]. However, none of the previous theoretical works appear to be highly accurate over various strengths of magnetic field because most of the wave functions are not guaranteed to converge to the exact wave function of the SE with the magnetic field.

According to the above stated situations of H_2^+ , highly accurate wave functions for the relativistic DE, the non-BO SE, and the SE under the magnetic field are desired for further development of the H_2^+ chemistry and physics. We have been working on these problems by our general, simple, and uniform methodology. In this review article, we summarize our theoretical studies on H_2^+ and its isotopomers performed with the Free-Complement (FC) methodology. First, we will briefly introduce our FC method that was introduced to solve the SE accurately and then we explain its applications to the non-relativistic, relativistic, and non-BO problems of H_2^+ . Finally, H_2^+ in magnetic field is addressed for its importance in astrophysics.

2. The Free-Complement method for solving the Schrödinger and Dirac equations

Recently, we have proposed and developed a general methodology for solving the SE in an analytical expansion form. We called this method as the Free-Complement (FC) method, and have been successfully applied to various atoms and molecules [56–80]. Such applications are realized by overcoming many difficulties that were existed before in solving the SE.

An important characteristic of our formalism lies in starting from the wave function having “exact structure”, so that it is guaranteed that the exact wave function is obtained at conver-

gence of our calculations. Next important feature is an overcome of the singularity difficulty, i.e. the divergence of higher-power integrals of Hamiltonian. This was done by introducing inverse Schrödinger equation (ISE) and the scaled Schrödinger equation (SSE), which are equivalent to the original SE [60,62]. Between the two, the SSE was simpler and easier to use for analytical calculations. This has enabled us to solve many atomic and molecular SE [65–68,71–78] or the relativistic DE or Dirac–Coulomb equations (DCE) [64,70,79,80], since these equations include singular Coulomb potentials. Some were actually the most accurate solutions so far obtained, not only for the energies but also for the satisfactions of the several conditions that the exact wave function must satisfy, such as the cusp conditions and the constancy of the local energy [67–69].

These results clearly show that the FC method gives extremely accurate wave functions that are guaranteed to converge to the exact wave function. In addition to its power to provide the exact wave function, another important character of the FC method is its wide applicability: The only one requirement for the applicability of the FC method is the existence of the analytical form of the Hamiltonian. Then, the Hamiltonian automatically generates the complement functions with which the exact wave functions are expanded. The undetermined parameters involved are calculated by applying the variation principle or by applying the local Schrödinger equation (LSE) method that is the integration-free method [69]. Due to its simplicity and generality, the FC method can be extended and applied to various types of problems in atomic and molecular physics and chemistry.

In the following, we briefly summarize how the FC method is employed to solve the SE and DE, focusing on the H_2^+ problems.

The SE is written as

$$H\psi - E\psi = 0. \quad (1)$$

The atomic or molecular Hamiltonian basically includes the Coulomb potential, which becomes infinite at particle coalescence points: this causes the singularity difficulty. This is avoided by introducing the SSE

$$g(H\psi - E\psi) = 0, \quad (2)$$

which is equivalent to the original SE [62,66]. The positive function $g(r)$ scales the singularities of the Coulomb potential to be finite.

Our basic idea is that the exact solution of the SE, DE, and DCE should be a function of its Hamiltonian, i.e. $\psi = f(H)\psi_0$, where ψ_0 is the initial function. Such sufficient functions that are guaranteed to become exact when solved by the variation method or other conditions equivalent to the SE, DE, and DCE (for example, LSE) are called to have “the exact structure”. A simple function that has the exact structure is the iterative complement (IC) function given by

$$\psi_{n+1} = [1 + C_n g(H - E_n)]\psi_n. \quad (3)$$

We call n as the FC order, which determines the quality of the FC wave function. This wave function is proved to become exact at convergence without encountering the singularity problem owing to the presence of the g function. We further generalized our method by collecting all the independent analytical functions on the rhs of Eq. (3) as $\{\phi_k\}^{(n)}$ ($k = 1, \dots, M_n$) and giving independent freedom (this is the origin of “free”) to each function ϕ_k , which we call “complement function”, as

$$\psi_{n+1} = \sum_{k=1}^{M_n} c_k \phi_k. \quad (4)$$

This is the FC wave function. The functions $\{\phi_k\}$ are called complement functions because they are the elements of the complete functions that expand the exact solution as expressed by Eq. (4).

Obviously, this formalism can be applied directly to other equations like the DE, the non-BO SE, and the SE under the external field [70,75,87].

In the FC formalism, we basically have two freedoms; the choice of the initial function (ψ_0) which is the starting function for the expansion of Eq. (3) and the choice of the g function. How to choose the proper initial function and the g function is not at all complicated; The initial function ψ_0 needs to be proper as a starting point in generating the exact wave function; for example, the initial function for solving the DE must be four-component spinor as the exact relativistic wave function must be. For the non-BO SE, the initial function should include the nuclear degrees of freedom so does the exact solution. The g function should be chosen as a functional of the inverse of the Coulomb potential, in order to eliminate its singularity. Note that one can reach the exact wave function with any selection of the g and initial functions. The convergence speed, however, depends on the selection.

Since the FC wave function is given as a sum of analytical functions (Eq. (4)), any properties can be calculated from them. One such property useful to examine the quality of the wave function is the variance of the energy given by

$$\sigma^2 = \frac{\langle \psi | H^2 | \psi \rangle}{\langle \psi | \psi \rangle} - \left[\frac{\langle \psi | H | \psi \rangle}{\langle \psi | \psi \rangle} \right]^2. \quad (5)$$

For the exact wave function, σ^2 becomes zero. In standard quantum chemistry, σ^2 is rarely calculated, seemingly because of the difficulty associated to the evaluation of H^2 integrals. Even if σ^2 is calculated, it would be meaninglessly bad when inaccurate wave function is employed. σ^2 is also important in practical sense since it is related to the lower bound of the energy; for details see Refs. [81–83]. In this paper, the energy lower bound is calculated according to the Temple's form [83] as

$$E_{\text{low}} = \langle \psi | H | \psi \rangle - \frac{\sigma^2}{E_{\text{ex}} - \langle \psi | H | \psi \rangle}, \quad (6)$$

where E_{ex} is the energy of the first excited state of the same symmetry as the ground state, and this is easily calculated by the FC method since the excited states are obtained, at the same time as the ground state, as the higher-energy solutions of the diagonalization. The energy lower bound is more important in the relativistic case than in the non-relativistic case, because the variational principle has problems in the DE or DCE cases.

Obvious from the above formalism, the FC method is quite simple and general, therefore can be extended to various types of problems. To see its wide applicability, H_2^+ is an excellent target because of its simplicity and abundance of experimental information. In this paper, we briefly summarize our calculations of H_2^+ employing the FC methodology. Our effort includes the non-relativistic and relativistic calculations, the non-BO calculation, and calculations under the magnetic field.

3. Solving the Schrödinger equation by the Free-Complement method

The SE of H_2^+ in the BO approximation (fixed nuclei SE) and without any external field is a good starting point for all the problems we will investigate in this paper. Furthermore, the exact solution is known in this case which enables the direct comparison between the exact wave function and our accurate wave function. Since both are given in infinite expansion forms, and both approach the true exact wave function, the point is which is easier and which converges faster.

In the following, we mention how to apply the FC method for solving the SE of H_2^+ in practice. The SE for H_2^+ is written in the form

of Eq. (1) and the Hamiltonian is given under the BO approximation as

$$H = -\frac{1}{2} \nabla_e^2 - \frac{1}{r_a} - \frac{1}{r_b} + \frac{1}{R}, \quad (7)$$

where a and b denote two nuclei, and R represents the internuclear distance. Throughout this paper, we use these notations. Owing to the BO approximation, this three-body problem is converted into a two-center one-particle problem, for which one favorably uses elliptic coordinate

$$\lambda = \frac{r_a + r_b}{R}, \quad \mu = \frac{r_a - r_b}{R}, \quad \omega. \quad (8)$$

In this coordinate, the kinetic operator is written as

$$-\frac{1}{2} \nabla_e^2 = -\frac{2}{R^2(\lambda^2 - \mu^2)} \left\{ \frac{\partial}{\partial \lambda} (\lambda^2 - 1) \frac{\partial}{\partial \lambda} + \frac{\partial}{\partial \mu} (1 - \mu^2) \frac{\partial}{\partial \mu} + \frac{(\lambda^2 - \mu^2)}{(\lambda^2 - 1)(1 - \mu^2)} \frac{\partial^2}{\partial \omega^2} \right\} \quad (9)$$

and the electron-nuclear Coulomb potential by

$$V = V_{\text{en}} = -\frac{4\lambda}{R(\lambda^2 - \mu^2)}. \quad (10)$$

As explained in the previous chapter, an important freedom associated with the FC method is the choice of the scaling function (g) and the initial function (ψ_0). Basically, the g function should be chosen so as to eliminate the singularity included in the Hamiltonian. In the current case, we choose it as the inverse of the electron-nuclear Coulomb potential. It is written in the elliptic coordinate as

$$g = -\frac{1}{V_{\text{en}}} = \frac{R(\lambda^2 - \mu^2)}{4\lambda}. \quad (11)$$

As for the initial function, we must employ the function that has the same symmetry as the electronic state we want to calculate. This is because the Hamiltonian is totally symmetric and does not change the symmetry of the wave function during the IC procedure. For the gerade state of H_2^+ , we employed the following Slater-type function as the initial function

$$\psi_0 = \exp[-\alpha'(r_a + r_b)] = \exp(-\alpha\lambda), \quad (12)$$

where α and α' are nonlinear parameters with $\alpha' = \alpha/R$. The ungerade state like $1\sigma_u$ can also be calculated when we choose the initial function as

$$\psi_0 = \mu \exp(-\alpha\lambda). \quad (13)$$

For both gerade and ungerade states, the g function is the same, since the singularity of Hamiltonian is common to all the electronic states.

Next, we move to computational results calculated by the FC method. First, we discuss the form of the FC functions automatically generated by the Hamiltonian. For the fixed nuclei SE, the above choice of g and ψ_0 gives the following form of the FC wave function

$$\psi = \sum_i c_i \lambda^{m_i} \mu^{n_i} \exp(-\alpha\lambda), \quad (14)$$

where c_i is the variational parameter and m_i is positive or negative integer. For the gerade states, n_i is zero or positive even integer and for the ungerade states, n_i is positive odd integer. This form of the wave function is similar to that by Hylleraas [8]. However, an important point is that the Hamiltonian generates not only the complement functions with the positive powers of λ ($m_i \geq 0$) but also those with the negative power of λ ($m_i < 0$). These functions take large value at the internuclear region, so our wave functions

are expected to be more accurate than the Hylleraas form particularly at the internuclear region.

Calculated energies for the $1\sigma_g$ and $1\sigma_u$ states are shown in Table 1 for different FC orders n . The dimension i.e. the number of complement functions, rapidly grows with increasing the FC order. This larger freedom of the higher order FC wave function enables the accurate solution toward the exact solution of the SE. In our experience, the convergence of the FC energy as n increases is quite good, and our best energies are better than previously calculated energies for both $1\sigma_g$ and $1\sigma_u$ states. This result clearly exhibits the convergence of the FC function toward the exact wave function.

In the SE, the convergence toward the exact wave function can be shown not only from the energy but also from the wave function itself. Note that this is possible for H_2^+ because its exact wave function is known for the fixed nuclei SE. So, we make a comparison between the FC and exact wave functions.

The exact wave function of H_2^+ in the BO approximation is given by [3,9–13]

$$\psi(\lambda, \mu, \omega) = \Lambda(\lambda)M(\mu) \exp(im\omega), \quad (15)$$

where

$$\Lambda(\lambda) = (1 + \lambda)^\sigma (\lambda^2 - 1)^{\frac{|m|}{2}} \exp(-\alpha\lambda) \sum_{k=0}^{\infty} g_k \left(\frac{1 - \lambda}{1 + \lambda} \right)^k$$

$$\sigma = \frac{R}{\alpha} - |m| - 1 \quad (16)$$

$$M(\mu) = \sum_{l=0}^{\infty} f_l P_l(\mu).$$

As seen from Eq. (16) this “exact” wave function also includes infinite number of analytical terms, similar to our FC wave function. In Eq. (16), m corresponds to the magnetic quantum number and zero for the $1\sigma_g$ state. $P_l(\mu)$ is associated Legendre function. g_k and f_l are the coefficients determined by the differential equations obtained from the SE by separating the variables. For the determination of these coefficients, we followed the method described by Hunter, Gray, and Pritchard [10]. In actual calculations using Eq. (16), we have to truncate at some order of λ and μ polynomials. Thus, we compare this “truncated exact” wave function with the FC wave function.

First, we calculated the wave function error defined as

$$\Delta = \int (\psi_{FC} - \psi_{\text{exact}})^2 d\tau, \quad (17)$$

where ψ_{FC} is the FC function, and ψ_{exact} is the truncated exact wave function in which maximum orders of λ and μ are taken as $\lambda_{\text{max}} = 23$ and $\mu_{\text{max}} = 14$, respectively. At different orders, $n = 1, 2$, and 3 , the Δ values were $\Delta = 1.07 \times 10^{-3}$, 2.49×10^{-6} , and

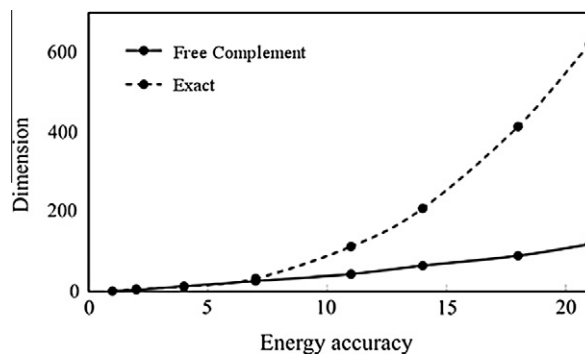


Fig. 1. The efficiency comparison between the FC and “exact” wave functions. The digits in x-axis is defined as the energy eigenvalue that has 10^{-N} (in a.u.) accuracy.

7.03×10^{-10} , respectively. These values show a rapid convergence of the FC wave function toward the exact wave function.

Interestingly, the exact wave function is given in the analytical expansion form in the “exact” form [3,9–13], and also as the FC wave function. Thus, the “exact” and FC expansions should be regarded as two different expression forms of the one unique exact wave function. So, a question arises; which is more efficient expansion for the exact wave function? To answer this, we estimated how many functions are necessary for obtaining the similar accuracy with the FC and the exact expansions. Fig. 1 shows a comparison between the truncated exact and the FC expansions to get the similar energy accuracy. The abscissa corresponds to the energy accuracy in the number of correct figures. Apparently, the convergence of the FC wave functions is faster and quite efficient. In addition, to calculate the truncated exact wave function, one must iteratively solve the eigenvalue equations and estimate the λ and μ truncation error. They are not an easy task as the dimension grows. Therefore, we could say that the FC procedure is much more efficient way of solving the non-relativistic exact wave function of H_2^+ than even the exact treatment of the SE of H_2^+ .

4. Solving the Dirac equation by the Free-Complement method

The SE of H_2^+ is efficiently solved by the FC method as shown in the previous chapter. The applicability of the FC method is not limited to the non-relativistic case at all [64,70,79,80]. In this chapter, we discuss the FC method applied to the relativistic DE of H_2^+ .

The extension to the relativistic DE is quite simple, since the DE is written in the form equivalent to the SE (Eq. (1)). In this case, the Hamiltonian is defined in a four-dimension matrix form as

$$H = \begin{bmatrix} (V + c^2)I_2 & c\boldsymbol{\sigma} \cdot \mathbf{p} \\ c\boldsymbol{\sigma} \cdot \mathbf{p} & (V - c^2)I_2 \end{bmatrix}, \quad (18)$$

Table 1

The convergence of non-relativistic energy (in a.u.) for $1\sigma_g$ and $1\sigma_u$ states of H_2^+ ($R = 2.0$ a.u.).

Order	Dimension	Energy	
		$1\sigma_g$ state	$1\sigma_u$ state
0	1	-1.079 384 965 831 435 080	-0.662 993 039 443 155 452
1	4	-1.101 421 270 731 672 256	-0.667 236 686 962 501 148
2	13	-1.102 627 432 357 876 892	-0.667 534 068 275 070 663
3	26	-1.102 634 208 423 548 446	-0.667 534 392 107 704 479
4	43	-1.102 634 214 493 685 465	-0.667 534 392 202 280 580
5	64	-1.102 634 214 494 945 584	-0.667 534 392 202 382 893
Our best result ($1\sigma_g$: order = 15, $1\sigma_u$: order = 14)		-1.102 634 214 494 946 462	-0.667 534 392 202 382 930
“Exact” wave function [9]		-1.102 634 214 494 9	-0.667 534 392 202 4
Finite element method [28]		-1.102 632 7	-0.667 533 1
Finite difference method [34]		-1.102 634 214 497	-0.667 534 392 205

where V is the same as the non-relativistic SE (Eq. (10)), and $\mathbf{p} = -i\nabla$ is the momentum operator, $\boldsymbol{\sigma}$ the Pauli matrix, and I_2 the 2×2 unit matrix. The speed of light is taken as $c = 1/\alpha = 137.0359895$ [84]. The wave function ψ here is four-component spinor.

Although the basic formalisms of the non-relativistic SE and the relativistic DE are equivalent, they have an important difference, that is, the variational property of the energy. In the non-relativistic case, the energy calculated by the variational procedure becomes upper bound to the exact energy, while in the relativistic case this no longer holds because of the presence of the positronic states in the DE. Many studies have been explored to overcome this problem [85]. Among them, we employed the inverse Hamiltonian method [60,86] in which the Ritz-type variational property is satisfied in a rigorous sense.

The variational collapse means also that the quality of the relativistic wave function cannot be identified just from the energy; the relativistic wave function with lower energy does not mean its better accuracy, unlike the non-relativistic case. For this reason, the energy lower bound is significantly important to examine the quality of the relativistic wave function. We also carried out the calculation of energy lower bounds according to Eq. (6).

Next, we discuss the choice of the g and initial functions. We selected the g function as

$$g = 1 - \frac{1}{V_{en}} = 1 + \frac{R(\lambda^2 - \mu^2)}{4\lambda} \quad (19)$$

in the relativistic calculations. Note that the g function is different from that of the non-relativistic SE (Eq. (11)). The unity in the g function is related to “the balancing condition” that the relativistic wave function should satisfy. The balancing condition only arises in the relativistic DE since it comes from the exact relationship between the large and small components of the wave function. Although the FC method can provide the exact relativistic wave function for any proper choice of the g function, we found that, in the relativistic case, the g function of Eq. (19) gives better convergence toward the exact wave function than the g function of Eq. (11); for detailed discussions, see our original paper [70].

In selecting the initial function, a notable difference from the non-relativistic case is that the wave function is composed of four components. The simplest initial function for the gerade and ungerade states would be

$$\psi_0 = \begin{bmatrix} \exp(-\alpha\lambda) \\ (\lambda^2 - 1)^{1/2} (1 - \mu^2)^{1/2} \exp(-\alpha\lambda) \exp(i\omega) \\ i \cdot \exp(-\alpha\lambda) \\ i \cdot (\lambda^2 - 1)^{1/2} (1 - \mu^2)^{1/2} \exp(-\alpha\lambda) \exp(i\omega) \end{bmatrix} \quad (20)$$

and

$$\psi_0 = \begin{bmatrix} \mu \exp(-\alpha\lambda) \\ (\lambda^2 - 1)^{1/2} (1 - \mu^2)^{1/2} \mu \exp(-\alpha\lambda) \exp(i\omega) \\ i \cdot \mu \exp(-\alpha\lambda) \\ i \cdot (\lambda^2 - 1)^{1/2} (1 - \mu^2)^{1/2} \mu \exp(-\alpha\lambda) \exp(i\omega) \end{bmatrix}, \quad (21)$$

respectively. Although accurate energies can be calculated with these initial functions [70], we employed, in actual calculations of the $1\sigma_g$ state, the initial function of

$$\psi_0 = \begin{bmatrix} \exp(-\alpha_1\lambda) + \exp(-\alpha_2\lambda) \\ (\lambda^2 - 1)^{1/2} (1 - \mu^2)^{1/2} \{\exp(-\alpha_1\lambda) + \exp(-\alpha_2\lambda)\} \exp(i\omega) \\ i \cdot \{\exp(-\alpha_1\lambda) + \exp(-\alpha_2\lambda)\} \\ i \cdot (\lambda^2 - 1)^{1/2} (1 - \mu^2)^{1/2} \{\exp(-\alpha_1\lambda) + \exp(-\alpha_2\lambda)\} \exp(i\omega) \end{bmatrix} \quad (22)$$

This is because we also need to calculate the first excited state ($2\sigma_g$) energy in order to have the energy lower bound of the ground $1\sigma_g$

state. The $2\sigma_g$ state is calculated at the same time as the ground $1\sigma_g$ state as the second lowest state. α_1 and $\alpha_2(=\alpha_1/2)$ in Eq. (22) correspond to the exponents of the ground and excited states, respectively.

Now we move to our computational results of the DE. First, we show the generated FC functions in the relativistic case. With the g and initial functions given above, the FC functions have the following form

$$\psi = \sum_i \begin{bmatrix} c_i^{(1)} \lambda^{m_i} \mu^{n_i} \exp(-\alpha\lambda) / (\lambda^2 - \mu^2)^{l_i} \\ c_i^{(2)} (\lambda^2 - 1)^{1/2} (1 - \mu^2)^{1/2} \lambda^{m_i} \mu^{n_i} \exp(-\alpha\lambda) \exp(i\omega) / (\lambda^2 - \mu^2)^{l_i} \\ i \cdot c_i^{(3)} \lambda^{m_i} \mu^{n_i} \exp(-\alpha\lambda) / (\lambda^2 - \mu^2)^{l_i} \\ i \cdot c_i^{(4)} (\lambda^2 - 1)^{1/2} (1 - \mu^2)^{1/2} \lambda^{m_i} \mu^{n_i} \exp(-\alpha\lambda) \exp(i\omega) / (\lambda^2 - \mu^2)^{l_i} \end{bmatrix}, \quad (23)$$

where $c_i^{(k)}$ ($k = 1, 2, 3, 4$) are variational parameters and m_i is positive or negative integer, l_i is positive integer. Likewise to the non-relativistic case, n_i is zero or positive even integer for the gerade state and positive odd integer for the ungerade state.

Relativistic energy upper and lower bounds for the $1\sigma_g$ state at different FC orders are shown in Table 2. Clearly, the upper and lower bounds converged to the exact energy from above and below, respectively. As the FC order increases, the width between the lower and upper bounds becomes narrower and narrower. Considering the fact that the lower bound corresponds to the variance of the energy, the present results indicate that a quite accurate wave function is obtained by the FC method. Not only the ground state but also the excited states of the DE can be easily calculated by the FC method; our best relativistic energies of the $1\sigma_u$ and $2\sigma_g$ states are **-0.667 552 771 995 5** and **-0.360 871 070 578 4** a.u., respectively. Throughout this paper, converged values are written in bold face. These energies are most accurate energies obtained so far. The detailed discussion of the excited state calculations can be found in our original paper [70].

Up to here, the energy calculations at the fixed geometries are shown. As the matter of fact, the FC method can be applied to arbitrary geometries since it provides the exact wave function in any case. This enables accurate calculations of the potential energy curve (PEC) by the FC method, as already provided for several molecules [69,78]. Here, the non-relativistic and relativistic PECs calculated by the FC method are discussed; numerical values of the PECs and details are given in a separate paper [87].

First, the relativistic effect, i.e. the energy difference between the non-relativistic and relativistic calculations is shown in Fig. 2 at different internuclear distance. As clearly seen in Fig. 2, the relativistic effect is large when R is small, while it gradually decreases as R increases, and take the minimum value at $R = 3.70$ a.u. However, it increases again for larger R . These results have shown that the relativistic effect is largest at the united atom limit, and

Table 2

Calculated energy upper and lower bounds (in a.u.) for the ground state ($1\sigma_g$) of H_2^+ with the g function given by Eq. (19) and the ψ_0 given by Eq. (22) ($R = 2.0$ a.u., $\alpha = 2.0$): The numbers of the spinor components are shown in parenthesis.

Order	Dimension	Upper bound	Lower bound
0	8 (2,2,2,2)	-0.943 164 843 437	-4924.519 845 377
1	40 (16,8,8,8)	-1.102 590 742 250	-1.953 823 274 365
2	186 (52,38,50,46)	-1.102 641 578 459	-1.102 654 667 382
3	392 (112,90,98,92)	-1.102 641 580 990	-1.102 642 557 369
4	672 (180,152,176,162)	-1.102 641 581 007	-1.102 642 197 633
5	1024 (282,244,252,246)	-1.102 641 581 015	-1.102 642 014 004
6	1448 (382,334,372,360)	-1.102 641 581 020	-1.102 641 881 501
7	1950 (524,468,484,474)	-1.102 641 581 023	-1.102 641 827 195
8	2524 (660,594,642,628)	-1.102 641 581 026	-1.102 641 777 580
Finite element method [28]			-1.102 641 581 033 8
Direct perturbation theory [29]			-1.102641579453
Monte Carlo method [30]			-1.102565
Minimax theory [32]			-1.102481

also large at the infinite separation limit. This result indicates that the relativistic effect is large when the electron density at nucleus is high, since the velocity of electron becomes larger and consequently, a larger relativistic effect is induced.

We also carried out the detailed calculation of the equilibrium distance (R_{eq}) of H_2^+ ; our calculations present that R_{eq} for non-relativistic and relativistic cases are 1.99719 and 1.99716 a.u., respectively. Therefore, the relativistic effect tends to shorten the chemical bond of H_2^+ by 3×10^{-5} a.u. The shorter chemical bond of H_2^+ in the relativistic case can be accounted from the electron density: the electron density difference between the relativistic and non-relativistic wave functions is shown in Fig. 3. Clearly, the electronic density is most different at the position of two nuclei. This also leads to the higher electron density in the internuclear region in the relativistic case, and accordingly, to a shorter chemical bond of H_2^+ in the relativistic case. These results also show that the electron density difference is quite small (order of 10^{-5} e), so that highly accurate wave function, like the FC wave function, is required to discuss the relativistic effect on the chemical bond of H_2^+ .

Next, based on these PECs, spectroscopic constants are evaluated. We calculated harmonic frequency (ω_g), anharmonicity constant ($\omega_g\chi_e$), rotational constant (B_e), and rotational–vibrational coupling constant (α_e), and transition frequency by using the extended Rydberg polynomial (ER) [88], extended Morse polynomial proposed by Hulbert and Hirschfelder (EM–HH) [89], and extended Morse polynomial proposed by Dunham (EM–D) [90,91]. The same PECs were also used to calculate rovibrational energy levels and spectroscopic constants for the isotopomers, HD^+ and HT^+ .

Non-relativistic and relativistic spectroscopic constants and their differences are summarized in Table 3. The relativistic effect tends to decrease ω_e when the EM-type polynomials were used, while ω_e is slightly increased when the ER-type polynomial was used. In contrast to ω_e , $\omega_g\chi_e$ is decreased by the relativistic effect with all polynomials, indicating that the anharmonicity is smaller for the relativistic PEC than for the non-relativistic one. The relativistic effects on the other two spectroscopic constants (α_e and B_e) are rather smaller than ω_e and $\omega_g\chi_e$. In contrast to the spectroscopic constants, the relativistic effect on the transition frequency is uniform irrespective of the fitting polynomials; in the relativistic calculations, the transition frequencies increased for all polynomials.

5. Non-Born–Oppenheimer calculation by the Free-Complement method

In the previous chapter, the SE and the DE with the BO approximation are accurately solved by the FC method. However, the FC

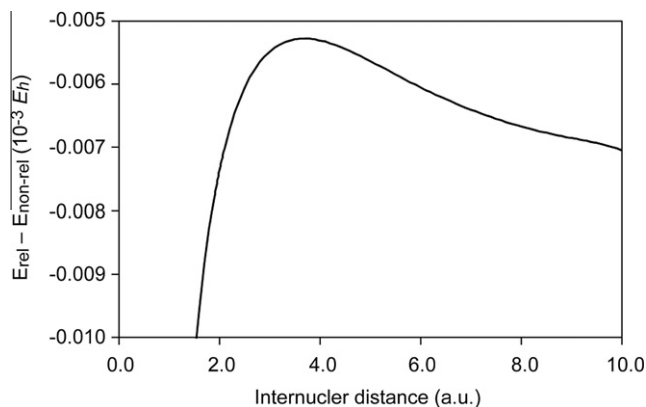


Fig. 2. The difference between the non-relativistic and the relativistic electronic energies along the different internuclear distances of H_2^+ . For calculations of potential energy curves, we employed the FC function of order = 4 in which 43 and 336 independent functions are included in non-relativistic and relativistic cases, respectively.

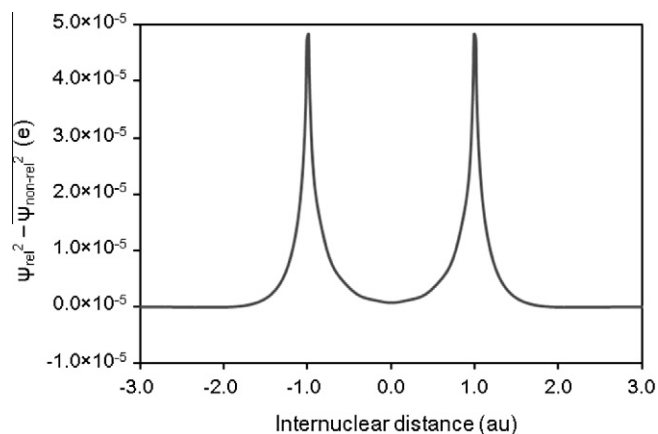


Fig. 3. Electronic density difference ($\psi_{rel}^2 - \psi_{non-rel}^2$) between relativistic and non-relativistic wave functions (order = 10, $R = 2.0$ a.u.) of H_2^+ . The three-dimensional electronic density is projected onto $(x, y) = (0, 0)$ plane and plotted along the z -axis.

method does not assume the BO approximation at all, and thus straightforwardly extended to the SE without assuming the BO approximation [75]. Note that the one-particle problem of H_2^+ in the non-BO case becomes three-particle problem in the non-BO case.

The non-BO Hamiltonian can be written in the general form as

$$H = - \sum_i \frac{1}{2m_e} \nabla_i^2 - \sum_A \frac{1}{2m_A} \nabla_A^2 + \sum_i \sum_A \frac{Z_e Z_A}{r_{iA}} + \sum_i \sum_{i < j} \frac{Z_e Z_e}{r_{ij}} + \sum_A \sum_{A < B} \frac{Z_A Z_B}{R_{AB}}, \quad (24)$$

where i and A denote electrons and nuclei, m_e and m_A their masses, and Z_e and Z_A their charges, respectively. After the center-of-mass motion is separated out, the Hamiltonian can be expressed by the interparticle coordinates (r_1, r_2, R) with angular factors. We introduce here the (s, t, R) coordinates for the present three-body systems, that is

$$s = r_1 + r_2, \quad t = r_1 - r_2, \quad R. \quad (25)$$

This coordinate set is equivalent to the (s, t, u) coordinate set for the helium atom used by Hylleraas [68,92].

Next, we discuss the choice of the g and initial functions. The g function appropriate for the non-BO SE is

$$-\frac{1}{V_{Ne}} + \frac{1}{V_{NN}} = \frac{s^2 - t^2}{4sZ} + R, \quad (26)$$

where V_{Ne} and V_{NN} represent nuclear–electronic attraction (with $Z = Z_1 = Z_2 = +1$) and nuclear–nuclear repulsion potentials, respectively.

In the non-BO calculation, we have to choose the initial function so as the generated FC functions properly describe the electronic and nuclear freedoms. For the nuclear part of the initial function, we employed the Gaussian function $\exp(-\gamma(R - R_e)^2)$, which would be proper as a vibrational function. In this case, the initial function ψ_0 for H_2^+ becomes

$$\begin{aligned} \psi_0 &= (1 + P_{12}) \left[\exp(-\alpha r_1) \exp(-\alpha r_2) \cdot \exp(-\beta(R - R_e)^2) \cdot Y_{LM}^{l_1, l_2} \right] \\ &= (1 + P_{12}) \left[\exp(-\alpha s) \cdot \exp(-\beta(R - R_e)^2) \cdot Y_{LM}^{l_1, l_2} \right], \end{aligned} \quad (27)$$

where P_{12} represents the permutation operator of two nuclei. α and β are nonlinear variational parameters and R_e is also a variational parameter but we fix it at $R_e = 2.0$ a.u. from the equilibrium distance of the nuclei of H_2^+ . (L, M, l_1, l_2) of $Y_{LM}^{l_1, l_2}$ is $(0, 0, 0, 0)$ for the ground states. For H_2^+ , because the proton is a fermion as is the electron,

Table 3
Non-relativistic and relativistic spectroscopic constants, transition frequencies, and zero-point energies (ZPE) (in cm^{-1}) of H_2^+ , HD^+ , and HT^+ . Upper, middle, and lower lines represent non-relativistic, relativistic, and their differences, respectively.

		ω_e	$\omega_g\chi_e$	α_e	B_e	Transition frequency			ZPE	
						0–1	1–2	2–3		
H_2^+	ER	2324.363	68.849	1.60332	29.95560	2190.43	2058.37	1921.02	1145.155	
		2324.378	68.613	1.60157	29.95623	2190.89	2060.33	1927.21	1145.211	
		0.014	–0.236	–0.00175	0.00063	0.46	1.95	6.19	0.056	
	EM–HH	2324.135	68.307	1.60100	29.95509	2191.19	2061.88	1932.01	1145.157	
		2323.928	67.741	1.59610	29.95506	2191.76	2064.62	1941.45	1145.164	
		–0.207	–0.566	–0.00490	–0.00003	0.57	2.74	9.44	0.007	
	EM–D	2323.941	67.994	1.60154	29.95488	2191.17	2061.46	1930.94	1145.118	
		2323.857	67.708	1.59779	29.95519	2191.44	2062.75	1935.61	1145.130	
		–0.084	–0.287	–0.00375	0.00031	0.26	1.29	4.68	0.012	
	Ref. [93]	2323.98	67.3	1.597	29.9626					
	Ref. [94]	2324.07	67.51	1.5962	29.9626					
	Ref. [95]					2191.13	2063.92			
	Exp. [96]	2321.8			29.8	2191.2	2064			
	HD^+	ER	2012.975	51.452	1.04085	22.46892	1912.65	1814.21	1713.65	993.747
2013.005			51.310	1.03995	22.46947	1912.92	1815.24	1716.93	993.791	
0.030			–0.142	–0.00090	0.00055	0.27	1.03	3.28	0.044	
EM–HH		2012.823	51.124	1.03964	22.46863	1913.04	1816.01	1719.41	993.739	
		2012.690	50.774	1.03687	22.46881	1913.32	1817.33	1724.15	993.739	
		–0.133	–0.350	–0.00277	0.00018	0.28	1.31	4.74	0.000	
EM–D		2012.692	50.933	1.03984	22.46851	1912.99	1815.64	1718.49	993.709	
		2012.641	50.748	1.03771	22.46888	1913.13	1816.27	1720.84	993.718	
		–0.051	–0.185	–0.00213	0.00037	0.14	0.63	2.35	0.009	
Ref. [95]						1913.00	1816.86			
Exp. [96]						1913.01	1816.7	1723.7		
HT^+		ER	1898.131	45.693	0.87252	19.97880	1808.95	1721.55	1632.78	937.745
			1898.165	45.577	0.87183	19.97931	1809.17	1722.35	1635.31	937.785
			0.034	–0.116	–0.00069	0.00051	0.22	0.80	2.53	0.040
	EM–HH	1897.954	45.278	0.86980	19.97823	1809.40	1723.78	1640.31	937.740	
		1897.891	45.136	0.86937	19.97879	1809.45	1723.88	1640.74	937.735	
		–0.064	–0.142	–0.00043	0.00056	0.05	0.10	0.43	–0.005	
	EM–D	1897.852	45.198	0.87078	19.97831	1809.18	1722.50	1636.29	937.702	
		1897.849	45.113	0.87001	19.97885	1809.31	1723.05	1638.12	937.717	
		–0.004	–0.086	–0.00077	0.00053	0.12	0.54	1.82	0.015	
	Ref. [95]					1809.22	1723.51			

the permutation symmetry of Eq. (27) (a plus sign before P_{12}) corresponds to the singlet state of ^1S .

We also calculated the triplet state ^3P with ψ_0 given by

$$\psi_0 = (1 - P_{12}) \left[(1 + t) \exp(-\alpha s) \cdot \exp(-\beta(R - R_e)^2) \cdot Y_{LM}^{l_1, l_2} \right] \quad (28)$$

with a minus sign before P_{12} and (L, M, l_1, l_2) of $(1, 0, 1, 0)$. The term $(1 + t)$ in Eq. (28) is introduced to generate additional spatial anti-symmetrized functions including odd powers of t . For the heteronuclear ions (HD^+ and HT^+), there is no need to symmetrize the wave function and so

$$\psi_0 = \exp(-\alpha s) \cdot \exp(-\beta(R - R_e)^2) \cdot Y_{LM}^{l_1, l_2} \quad (29)$$

is employed with $R_e = 2.0$ a.u. and $Y_{LM}^{l_1, l_2}: (0, 0, 0, 0)$.

Not only the vibronic ground state but also the vibronic excited states can be calculated simultaneously. A few vibronic excited states are also calculated as second and third solutions in the diagonalization process.

Next, we discuss the computational results of the non-BO calculations. The FC functions generated from the g and ψ_0 of Eqs. (26)–(29) are expressed as

$$\psi = (1 \pm P_{12}) \sum_{(i,j,k)} s^i t^j R^k \exp(-\alpha s) \cdot \exp(-\beta(R - R_e)^2) \cdot Y_{LM}^{l_1, l_2}, \quad (30)$$

where both i and k run over integers including negative integers, and the index j runs only over nonnegative even integers for the ground state of H_2^+ . For HD^+ and HT^+ , in addition to the even integers of j , the wave function also involves odd-integer powers of t derived from the heterosymmetric Hamiltonian.

Calculated non-BO energies of the 1^1S and 1^3P states are shown in Table 4. For the 1^1S and the 1^3P states, we obtained our best energy of **–0.597 139 063 123 405 074 834 134 096 025 974 142** and **–0.596 873 738 832 764 735 920 744 893** a.u. for the 1^1S and 1^3P states, respectively. Comparing these energies with the previous works, they should be regarded as the best energy. The energy difference between the 1^1S and 1^3P states was calculated to be 0.000 265 324 a.u. ($58.231\ 941\ \text{cm}^{-1}$).

Since we have quite accurate wave function in analytic form, any properties other than energy can be calculated in extreme accuracy. A good example to investigate the nature of the non-BO wave function is the reduced density function $f(R)$ which is defined by

$$f(R) = \int \psi^* \psi d\tau_R^*, \quad (31)$$

where $d\tau_R^*$ means that the integrations are over the coordinates except for the internuclear distance, R . Therefore, the rhs of Eq. (31) becomes a function of R and can be expressed as

$$f(R) = \sum_k C_k R^k e^{-2\beta R^2 - (2\alpha - 4\beta R_e)R}. \quad (32)$$

Fig. 4 shows the plots of $f(R)$ for the ground, first, and second excited states of ^1S H_2^+ . We compare them with the densities calculated from the vibrational wave function of the harmonic oscillator on the BO potential curve. For the ground and second excited states, the number of maximum peaks is odd and the plots are roughly symmetric about the central peak position (which should be very close to the equilibrium distance), i.e., the gerade mode of the vibra-

Table 4

The convergence of non-Born–Oppenheimer energy (in a.u.) of H_2^+ in 1^1S and 1^3P states. The g function of Eq. (26) is used, and ψ_{0S} are Eqs. (27) and (28) for 1^1S and 1^3P states, respectively. The proton mass $m_H = 1836.152\,701$ was used to compare with the previous reference.

Order	1^1S state		1^3P state	
	Dimension	Energy	Dimension	Energy
0	1	−0.573 217	2	−0.534 562
1	7	−0.596 661	16	−0.596 331
2	30	−0.597 133 402	66	−0.596 870 838
3	83	−0.597 139 017 109	180	−0.596 873 713 262
4	179	−0.597 139 062 391	378	−0.596 873 738 458
5	330	−0.597 139 063 103 997	690	−0.596 873 738 824 230
		⋮		⋮
10	2273	−0.597 139 063 123 405 073 177	4656	−0.596 873 738 832 764 735 144
11	2981	−0.597 139 063 123 405 074 767	6094	−0.596 873 738 832 764 735 875
12	3822	−0.597 139 063 123 405 074 831 055	7800	−0.596 873 738 832 764 735 917 782
13	4808	−0.597 139 063 123 405 074 833 976	9798	−0.596 873 738 832 764 735 920 539
14	5950	−0.597 139 063 123 405 074 834 125 011	12110	−0.596 873 738 832 764 735 920 730
15	7260	−0.597 139 063 123 405 074 834 133 503	14760	−0.596 873 738 832 764 735 920 743 846
Our best result	19,286 (order = 21)	−0.597 139 063 123 405 074 834 134 096 025	17,770 (order = 16)	−0.596 873 738 832 764 735 920 744 893
Ref. [40]		−0.597 139 063 123 405 074 834 134 096 021		−0.596 873 738 832 764 735 920 744 98

tion. In contrast, for the first excited state, the number of maximum peaks is even and the plot is roughly antisymmetric, i.e., the ungerade mode. Obviously, the plots for the harmonic oscillator are completely symmetric about the minimum position of the harmonic potential but the plots from the present non-BO calculations are not completely symmetric and are distorted because of the anharmonicity of the vibrational motion and the non-BO effects, which come from the coupling of electron and nuclei motions. Unsurpris-

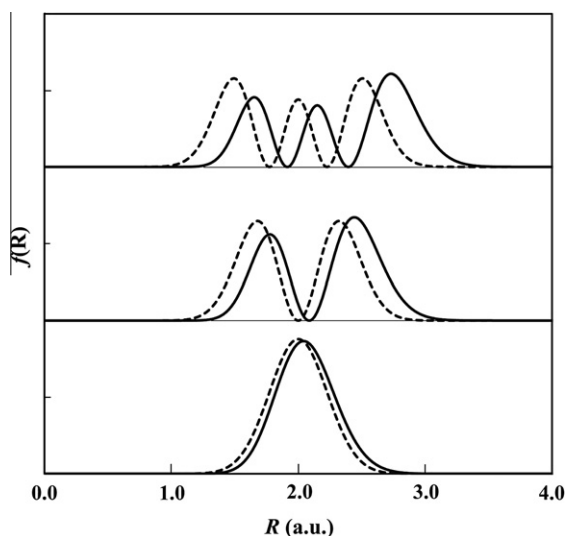


Fig. 4. Plots of the reduced density given by Eq. (31) for the ground and vibronic excited states of H_2^+ of 1^1S symmetry. The solid lines represent the reduced density functions of the ground, first, and second excited states from the bottom. The dotted lines represent the density plots for the harmonic vibrational wave functions.

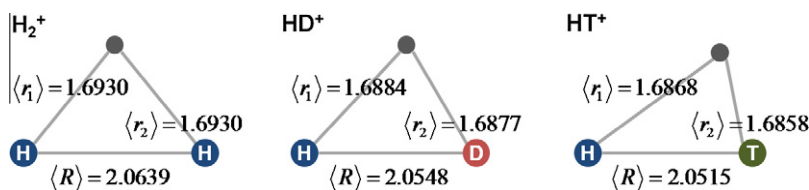


Fig. 5. Expectation values of nucleus–electron distances (r_1, r_2) and internuclear distance (R) of H_2^+ (1^1S), HD^+ , and HT^+ molecules. The g function of Eq. (26) is used, and ψ_0 's are Eqs. (27) and (29) for homo- and hetero-nuclear molecules, respectively. Calculated values are those of order = 14 and 11 for homo- and hetero-nuclear molecules, respectively. The nuclear mass data used were $m_H = 1836.152\,672\,47$, $m_D = 3670.482\,9654$, and $m_T = 5496.921\,5269$.

ingly, the anharmonicity is automatically included in the non-BO calculations.

Another important properties calculated from the non-BO wave function is the expectation values of $\langle r_1 \rangle$, $\langle r_2 \rangle$, and $\langle R \rangle$. Here, for heteronuclear systems, r_1 is defined as the distance between the electron and the lighter nucleus and r_2 as the distance between the electron and the heavier nucleus. These expectation values are interesting properties to be compared among the isotopomers. $\langle r_1 \rangle$, $\langle r_2 \rangle$, and $\langle R \rangle$ values of H_2^+ , HD^+ , and HT^+ calculated by the FC method are summarized in Fig. 5. $\langle r_1 \rangle$ and $\langle r_2 \rangle$ values were slightly less than 1.7 a.u. for the ground states of all the systems. Although the Coulomb potentials are the same for both homo- and heteronuclear systems, $\langle r_1 \rangle$ (the electron–light nucleus distance) is slightly larger than $\langle r_2 \rangle$ (the electron–heavy nucleus distance) for HD^+ and HT^+ . These results indicate that the electron tends to be more attracted to the heavier nucleus. The electron near the heavier nucleus is more stable because the heavier nucleus does not easily move or flicker because of its heavy weight, so that the electron can exist nearer the heavier nucleus than near the lighter nucleus. The expectation value for the internuclear distance $\langle R \rangle$ is close to 2.0 a.u. for the ground states of all the systems, which is very close to the equilibrium distance obtained from the BO calculations. This value of $\langle R \rangle$ becomes slightly shorter as the nuclear mass becomes heavier for the same reason as those for $\langle r_1 \rangle$ and $\langle r_2 \rangle$, which can never be explained in the BO approximation.

6. Solving the Schrödinger equation under the magnetic field by the Free-Complement method

In this chapter, we see that the FC method can also be applied to the SE under the external field, where various physically and chemically interesting phenomena take place [55,79,80]. The SE with external field provides another example in which the exact

wave function is not known although the analytical form of the Hamiltonian is uniquely defined. Here, the FC method is applied to the SE of H_2^+ under the magnetic field, with various strengths and directions of the field [87].

The SE of H_2^+ under the magnetic field has the following Hamiltonian

$$H = \frac{1}{2}[-i\nabla + \mathbf{A}(\mathbf{r})]^2 - \left[\frac{1}{r_a} + \frac{1}{r_b} \right] + \frac{1}{R}, \quad (33)$$

where $\mathbf{A}(\mathbf{r})$ represents the external vector potential. When the system possesses a rotational symmetry, one favorably use the symmetric gauge and in this case [54,55]

$$\mathbf{A}(\mathbf{r}) = \frac{1}{2}(\mathbf{B} \times \mathbf{r}), \quad (34)$$

where \mathbf{B} is the magnetic field vector. For the direction of the magnetic field, we choose two extreme cases, either parallel or perpendicular to the molecular axis. Parallel and perpendicular magnetic fields are written in Cartesian coordinate as

$$\mathbf{B} = [0 \quad 0 \quad B]^T \quad (35)$$

and

$$\mathbf{B} = [B \quad 0 \quad 0]^T, \quad (36)$$

respectively, where we assume the internuclear axis is along the z -axis.

Here, our main interest is a moderate magnetic field strength in which chemical interests often appears. In this case, we can choose the same initial function as in the field-free case, that is,

$$\psi_0 = \exp(-\alpha\lambda) \quad (37)$$

for both parallel and perpendicular cases. We also take the same g function as in the field-free case (Eq. (11)), because no additional singularity arises from the magnetic field part.

Next, we discuss our computational results. In the parallel field, the generated FC wave function form can be written as

$$\psi = \sum_i c_i \lambda^{m_i} \mu^{n_i} \exp(-\alpha\lambda), \quad (38)$$

where c_i is a variational parameter and m_i is a positive or negative integer. The index n_i is zero or positive even integer for the gerade states. This wave function form is the same as for the field-free case (Eq. (14)), however, the number of functions is larger since $\mathbf{A}(\mathbf{r})$ contributes to the wave function generation.

The generated FC wave function form for the perpendicular field is, on the other hand,

$$\psi = \sum_i c_i \lambda^{m_i} \mu^{n_i} (\lambda^2 - 1)^{\frac{M}{2}} (1 - \mu^2)^{\frac{M}{2}} \exp(-\alpha\lambda) \exp(iM\omega), \quad (39)$$

where M is the magnetic angular momentum quantum number. In Eq. (39), the range of n_i index is related to M ; n_i is zero or even positive integer for even M , and odd positive integer for odd M . The perpendicular field FC function is different from the parallel field one because the rotational symmetry with respect to the internuclear axis is no longer held in the perpendicular field. Thus, M is no longer a good quantum number so that the exact wave function would be the mixture of the functions with various M numbers. Interestingly, the expansion by M is automatically introduced, in the complement function generation step, by the perpendicular field Hamiltonian, even though the same initial function (Eq. (37)) was employed.

Ground state total energies of H_2^+ in various strengths of parallel and perpendicular magnetic fields are summarized in Table 5. Despite of the simplicity of the initial function, our results are impressive in all the calculated cases. The calculated energies are more accurate in weak fields than in strong fields, reflecting the form of the initial function. However, when sufficient FC order is employed, the wave function becomes accurate even in strong fields. Our calculated energies are variational in all cases and some of them are of the lowest energies so far obtained.

It is well known that the vector potential for a given magnetic field is defined ambiguously up to a gradient of an arbitrary scalar function. In addition, there is another ambiguity where to set the gauge-origin, i.e. the point where the vector potential vanishes. In H_2^+ under the parallel magnetic field, as long as the symmetric gauge is employed (Eq. (34)), the calculated energies are invariant to the gauge-origin. On the other hand, in the perpendicular case, the calculated energy depends on the gauge-origin. This fact gives rise to the gauge-origin dependence of the observables. In fact, this provides another condition that the exact wave function should satisfy, that is, the observables are invariant to the gauge-origin if the employed wave function is truly exact.

So, we investigate here the gauge-origin dependence of the FC function with two different cases; (i) the gauge-origin is placed on the midpoint of two nuclei, and (ii) the gauge-origin is placed on one nucleus. The Hamiltonian of the former and later cases are denoted as H_{mid} and H_{nuc} , respectively. Note that the parallel

Table 5
Total energy (in a.u.) for the ground state ($1\sigma_g$) of H_2^+ in the parallel and perpendicular magnetic fields (1 a.u. = 2.35×10^9 G).

	Order	Dimension	Magnetic field strength			
			10^9 G	1 a.u.	10^{10} G	10 a.u.
Parallel field	0	1	-0.481 976	-0.235 391	4.491	26.067
	1	8	-0.574 840	-0.474 946	0.682 748	3.281
	2	36	-0.575 358 923 943	-0.474 987 590	0.545 783	2.832
	3	81	-0.575 358 927 862 336	-0.474 988 243 105	0.545 159 616	2.825 200
	4	144	-0.575 358 927 863 067	-0.474 988 244 639	0.545 151 266	2.825 017
	Our best result (order = 10)	900	-0.575 358 927 863 071	-0.474 988 244 647	0.545 151 122	2.825 014
	Ref. [51]		-0.575 36		0.545 155	2.825
	Ref. [54]		-0.575 35	-0.474 955	0.545 22	2.825 12
Perpendicular field	0	1	-0.475 518	-0.209 312	4.615	26.212
	1	14	-0.568 376	-0.443 555	0.913 907	3.793
	2	122	-0.569 154 452 429	-0.450 622 627	0.689 428	3.203
	3	421	-0.569 154 949 854 049	-0.450 684 160 814	0.679 744 557	3.141 846
	4	1016	-0.569 154 952 148 180	-0.450 685 613 141	0.678 475 853	3.119 157
	Our best result (order = 6)	3510	-0.569 154 952 168 045	-0.450 685 661 585	0.678 045 524	3.111 913
	Ref. [51]		-0.569 160		0.678 060	
	Ref. [54]		-0.568 671	-0.449 555	0.681 035	3.115 85

Table 6

Total energy (in a.u.) for the ground state ($1\sigma_g$) of H_2^+ in the perpendicular magnetic field where gauge-origin is placed on one of two nuclei (H_{nuc} Hamiltonian) (1 a.u. = 2.35×10^9 G).

Magnetic field	10^9 G	1 a.u.	10^{10} G	10 a.u.
Internuclear distance (a.u.)	1.875	1.635	1.059	0.772
Order	Dimension			
0	1	−0.433	−0.291	1.715
1	18	−0.564 825	−0.443	1.026
2	190	−0.569 153 2	−0.450 553	0.707
3	726	−0.569 154 949	−0.450 681 06	0.684
4	1828	−0.569 154 952 133	−0.450 685 38	0.679 060
5	3704	−0.569 154 952 167 4	−0.450 685 639	0.678 254
Ref. [54]		−0.568 671	−0.449 555	0.681 035
H_{mid}		−0.569 154 952 168 020	−0.450 685 661	0.678 045

and perpendicular field calculations up to here correspond to the calculations employing the H_{mid} Hamiltonian.

The perpendicular field FC function generated by the H_{nuc} can be written as follows;

$$\psi = \sum_i c_i \lambda^{m_i} \mu^{n_i} (\lambda^2 - 1)^{\frac{M}{2}} (1 - \mu^2)^{\frac{M}{2}} \exp(-\alpha\lambda) \exp(iM\omega), \quad (40)$$

where m_i and n_i are positive and negative integer. We employed the g and initial functions of Eqs. (14) and (37), respectively. Notable difference with the perpendicular field FC function generated by H_{mid} (Eq. (39)) is that odd number of n_i is allowed for all M numbers. This is because, for H_{nuc} case, mirror symmetry is broken because the gauge-origin is placed at one nucleus. The wave function form of Eq. (40) reflects that this symmetry-breaking is automatically taken into account by the H_{nuc} Hamiltonian, even when we start from the simple initial function.

Next, ground state total energies with different gauge-origins are compared in Table 6. At smaller FC orders such as $n = 1$, the calculated energies are dependent on the gauge-origin. However, when the FC order is increased, energy differences decrease substantially; for example, at 10^9 G, energy difference between H_{mid} and H_{nuc} is 4.33×10^{-3} a.u. at $n = 1$, while it decreases to 6.02×10^{-13} a.u. at $n = 5$. These results show that the wave function provided by the FC method converges towards the exact wave function, also from the viewpoint of the gauge-origin.

7. Conclusions

In this paper, we have summarized our theoretical investigations on H_2^+ using the potentially exact wave function generated by the FC method. Our works include the non-relativistic SE, relativistic DE, the non-BO problem, and the SE under the magnetic field. We have successfully shown that the FC method combined with the variational principle gives very accurate analytical wave functions of H_2^+ in all the cases.

For all the examples discussed in this paper, the FC method provides successful results because the wave function form suitable for the problem is automatically generated by the Hamiltonian of the equation we want to solve. More importantly, these wave functions are potentially exact, i.e. they are guaranteed to converge toward the exact wave function. This character is indeed strong when the exact wave function form is not known, such as the DE, the non-BO SE, and the SE under the magnetic field.

In this paper, we employed the FC method combined with the variational principle because analytical integrations over the FC functions are possible. For larger atoms and molecules, such integrations are no longer possible. To overcome this “integration difficulty”, we proposed the local Schrödinger equation (LSE) method [69], and we expect that the FC method combined with the LSE would be the dominant approach to provide the analytical solution

of the SE, DE, and DCE in various situations and approximations (like the BO approximation).

Acknowledgments

This is a contribution to the special issue dedicated to Prof. Debashis Mukherjee to celebrate his 65th birthday. H.N. wants to express his sincere congratulations for the long-lasting seminal contributions of Prof. Mukherjee to theoretical quantum chemistry.

References

- [1] C.A. Leach, R.E. Moss, *Annu. Rev. Phys. Chem.* 46 (1995) 55.
- [2] A. Carrington, I.R. McNab, C.A. Montgomery, *J. Phys. B: Atom. Mol. Opt. Phys.* 22 (1989) 3551.
- [3] C. Jaffé, *Z. Phys.* 87 (1934) 535.
- [4] V. Guillemin, C. Zener, *Proc. Natl. Acad. Sci. US* 15 (1929) 314.
- [5] A. Dalgarno, G. Poots, *Proc. Phys. Soc. (London)* 67A (1954) 343.
- [6] H.M. James, *J. Chem. Phys.* 3 (1935) 9.
- [7] B.N. Dickinson, *J. Chem. Phys.* 1 (1933) 317.
- [8] E.A. Hylleraas, *Z. Phys.* 71 (1931) 739.
- [9] H. Wind, *J. Chem. Phys.* 42 (1965) 2371.
- [10] G. Hunter, B.F. Gray, H.O. Pritchard, *J. Chem. Phys.* 45 (1966) 3806.
- [11] G. Hunter, H.O. Pritchard, *J. Chem. Phys.* 46 (1967) 2146.
- [12] G. Hunter, H.O. Pritchard, *J. Chem. Phys.* 46 (1967) 2153.
- [13] J.M. Peek, *J. Chem. Phys.* 43 (1965) 3004.
- [14] W.H. Wing, G.A. Ruff, W.E. Lamb, J.J. Spezeski, *Phys. Rev. Lett.* 36 (1976) 1488.
- [15] Y.P. Zhang, C.H. Cheng, J.T. Kim, J. Stanojevic, E.E. Eyler, *Phys. Rev. Lett.* 92 (2004) 203003.
- [16] R. Herman, R.F. Wallis, *Astrophys. J.* 123 (1956) 353.
- [17] V.K. Khersonskii, *Astrophys. Space Sci.* 98 (1984) 255.
- [18] V.K. Khersonskii, *Astrophys. Space Sci.* 103 (1984) 357.
- [19] D.R. Bringham, J.M. Wadehra, *Astrophys. J.* 317 (1987) 865.
- [20] V.K. Khersonskii, *Astrophys. Space Sci.* 117 (1985) 47.
- [21] D. Sanwal, G.G. Pavlov, V.E. Zavlin, M.A. Teter, *Astrophys. J.* 574 (2002) L61.
- [22] G.F. Bignami, P.A. Caraveo, A. De Luca, S. Mereghetti, *Nature* 423 (2003) 725.
- [23] M.H. van Kerkwijk, D.L. Kaplan, M. Durant, S.R. Kulkarni, F. Paerels, *Astrophys. J.* 608 (2004) 432.
- [24] J. Vink, C.P. de Vries, M. Mendrez, F. Verbunt, *Astrophys. J.* 609 (2004) L75.
- [25] K. Mori, J. Chonko, C.J. Hailey, *Astrophys. J.* 631 (2005) 1082.
- [26] C.J. Hailey, K. Mori, *Astrophys. J.* 578 (2002) L133.
- [27] B.K. Bhaduri, Y. Nogami, C.S. Varke, *Astrophys. J.* 217 (1977) 324.
- [28] O. Kullie, D. Kolb, *Eur. Phys. J. D* 17 (2001) 167.
- [29] R. Franke, W. Kutzelnigg, *Chem. Phys. Lett.* 199 (1992) 561.
- [30] S.A. Alexander, R.L. Coldwell, *Phys. Rev. E* 60 (1999) 3374.
- [31] F.A. Parpia, A.K. Mohanty, *Chem. Phys. Lett.* 238 (1994) 209.
- [32] L. La John, J.D. Talman, *Chem. Phys. Lett.* 189 (1992) 383.
- [33] O. Kullie, D. Kolb, A. Rutkowski, *Chem. Phys. Lett.* 383 (2004) 215.
- [34] L. Laaksonen, P. Pyykko, D. Sundholm, *Int. J. Quantum Chem.* 23 (1983) 309.
- [35] L. Yang, D. Heinemann, D. Kolb, *Phys. Rev. A* 48 (1993) 2700.
- [36] R.E. Moss, *J. Phys. B* 32 (1999) L89.
- [37] L. Hilico, N. Billy, B. Grémaud, D. Delande, *Eur. Phys. J. D* 12 (2000) 449.
- [38] D.H. Bailey, A.M. Frolov, *J. Phys. B* 35 (2002) 4287.
- [39] M.M. Cassar, G.M.F. Drake, *J. Phys. B* 37 (2004) 2485.
- [40] H. Li, J. Wu, B.-L. Zhou, J.-M. Zhu, Z.-C. Yan, *Phys. Rev. A* 75 (2007) 012504.
- [41] S. Bubin, L. Adamowicz, *Chem. Phys. Lett.* 403 (2005) 185.
- [42] S. Bubin, E. Bednarsz, L. Adamowicz, *J. Chem. Phys.* 122 (2005) 041102.
- [43] E. Bednarsz, S. Bubin, L. Adamowicz, *J. Chem. Phys.* 122 (2005) 164302.
- [44] R. Jaquet, W. Kutzelnigg, *Chem. Phys.* 346 (2008) 69.
- [45] J.C. de Melo, T.K. Das, R.C. Ferreira, L.C.M. Miranda, H.S. Brandi, *Phys. Rev. A* 18 (1978) 12.
- [46] C.P. de Melo, R. Ferreira, H.S. Brandi, L.C.M. Miranda, *Phys. Rev. Lett.* 37 (1976) 676.

- [47] C.S. Lai, *Can. J. Phys.* 55 (1977) 1013.
- [48] C.S. Lai, B. Suen, *Can. J. Phys.* 55 (1977) 609.
- [49] C.S. Warke, A.K. Dutta, *Phys. Rev. A* 16 (1977) 1747.
- [50] J.M. Peek, J. Katriel, *Phys. Rev. A* 21 (1980) 413.
- [51] U. Wille, *Phys. Rev. A* 38 (1988) 3210.
- [52] M.S. Kaschiev, S.I. Vinitsky, F.R. Vukajlovic, *Phys. Rev. A* 22 (1980) 557.
- [53] A.V. Turbiner, J.C. Lopez Vieyra, *Phys. Rev. A* 68 (2003) 012504.
- [54] A.V. Turbiner, J.C. Lopez Vieyra, *Phys. Rev. A* 69 (2004) 053413.
- [55] A.V. Turbiner, J.C. Lopez Vieyra, *Phys. Rep.* 424 (2006) 309.
- [56] H. Nakatsuji, *J. Chem. Phys.* 113 (2000) 2949.
- [57] H. Nakatsuji, E.R. Davidson, *J. Chem. Phys.* 115 (2001) 2000.
- [58] H. Nakatsuji, *J. Chem. Phys.* 115 (2001) 2465.
- [59] H. Nakatsuji, *J. Chem. Phys.* 116 (2002) 1811.
- [60] H. Nakatsuji, *Phys. Rev. A* 65 (2002) 052122.
- [61] H. Nakatsuji, M. Ehara, *J. Chem. Phys.* 117 (2002) 9.
- [62] H. Nakatsuji, *Phys. Rev. Lett.* 93 (2004) 030403.
- [63] H. Nakatsuji, *Bull. Chem. Soc. Jpn.* 78 (2005) 1705.
- [64] H. Nakatsuji, H. Nakashima, *Phys. Rev. Lett.* 95 (2005) 050407.
- [65] H. Nakatsuji, M. Ehara, *J. Chem. Phys.* 122 (2005) 194108.
- [66] H. Nakatsuji, *Phys. Rev. A* 72 (2005) 062110.
- [67] Y. Kurokawa, H. Nakashima, H. Nakatsuji, *Phys. Rev. A* 72 (2005) 062502.
- [68] H. Nakashima, H. Nakatsuji, *J. Chem. Phys.* 127 (2007) 224104.
- [69] H. Nakatsuji, H. Nakashima, Y. Kurokawa, A. Ishikawa, *Phys. Rev. Lett.* 99 (2007) 240402.
- [70] A. Ishikawa, H. Nakashima, H. Nakatsuji, *J. Chem. Phys.* 128 (2008) 124103.
- [71] H. Nakashima, H. Nakatsuji, *J. Chem. Phys.* 128 (2008) 154107.
- [72] H. Nakashima, Y. Hijikata, H. Nakatsuji, *J. Chem. Phys.* 128 (2008) 154108.
- [73] Y. Kurokawa, H. Nakashima, H. Nakatsuji, *Phys. Chem. Chem. Phys.* 10 (2008) 4486.
- [74] H. Nakashima, H. Nakatsuji, *Phys. Rev. Lett.* 101 (2008) 240406.
- [75] Y. Hijikata, H. Nakashima, H. Nakatsuji, *J. Chem. Phys.* 130 (2009) 024102.
- [76] H. Nakatsuji, H. Nakashima, *Int. J. Quant. Chem.* 109 (2009) 2248.
- [77] H. Nakatsuji, H. Nakashima, *Advances in the Theory of Atomic and Molecular Systems* 19 (2009) 47.
- [78] A. Bande, H. Nakashima, H. Nakatsuji, *Chem. Phys. Lett.* 496 (2010) 347.
- [79] H. Nakashima, H. Nakatsuji, *Astrophys. J.* 725 (2010) 528.
- [80] H. Nakashima, H. Nakatsuji, *Theoret. Chem. Acc.* 129 (2011) 567.
- [81] F. Weinhold, *J. Math. Phys.* 11 (1970) 2127.
- [82] A.F. Stevenson, M.F. Crawford, *Phys. Rev.* 54 (1938) 375.
- [83] G. Temple, *Proc. Roy. Soc. A* 119 (1928) 276.
- [84] W.E. Baylis, G.W.F. Drake, in: G.W.F. Drake (Ed.), *Atomic, Molecular, & Optical Physics Handbook*, AIP Press, New York, 1996.
- [85] W. Kutzelnigg, *Chem. Phys.* 225 (1997) 203.
- [86] R.N. Hill, C. Krauthauser, *Phys. Rev. Lett.* 72 (1994) 2151.
- [87] A. Ishikawa, H. Nakashima, H. Nakatsuji, in preparation.
- [88] P. Huxley, J.N. Murrell, *J. Chem. Soc., Faraday Trans.* 79 (1983) 323.
- [89] H.M. Hulbert, J.O. Hirschfelder, *J. Chem. Phys.* 9 (1941) 61.
- [90] J.L. Dunham, *Phys. Rev.* 41 (1932) 721.
- [91] J.L. Dunham, *Phys. Rev.* 41 (1932) 713.
- [92] E.A. Hylleraas, *Z. Phys.* 54 (1929) 347.
- [93] S.A. Alexander, R.L. Coldwell, *Chem. Phys. Lett.* 413 (2005) 253.
- [94] C.L. Beckel, B.D. Hansen, J.M. Peek, *J. Chem. Phys.* 53 (1970) 3681.
- [95] D.M. Bishop, L.M. Cheung, *Phys. Rev. A* 16 (1977) 640.
- [96] K.P. Huber, G. Herzberg, *Molecular Spectra Molecular Structure IV. Constants of Diatomic Molecules*, Van Nostrand, Reinhold, New York, 1979.